Bulletin of Electrical Engineering and Informatics
Vol. 14, No. 2, April 2025, pp. 1054~1062
ISSN: 2302-9285, DOI: 10.11591/eei.v14i2.8533

A 0.7 GHz and 0.9 GHz efficient and compact dual-band rectifier for ambient radio frequency energy harvesting

Raja Nor Azrin Raja Yunus[1], Ismahayati Adam[1,2], Mohd Najib Mohd Yasin[1,2], Surajo Muhammad[3], Wan Zuki Azman Wan Muhamad[4], Abdulrahman Amin Ahmed Ghaleb[1]
[1]Faculty of Electronic Engineering and Technology, Universiti Malaysia Perlis, Arau, Perlis, Malaysia
[2]Centre of Excellence for Advanced Communication Engineering, Universiti Malaysia Perlis, Arau, Perlis, Malaysia
[3]Department of Electronics and Telecommunication, Ahmadu Bello University, Zaria, Nigeria
[4]Institute of Engineering Mathematics, Universiti Malaysia Perlis, Arau, Malaysia

Article Info

Article history:

Received Apr 1, 2024
Revised Nov 8, 2024
Accepted Nov 19, 2024

Keywords:

5G application
Impedance matching network
Power conversion efficiency
Radio frequency energy harvesting
Rectifier

ABSTRACT

This study introduces a compact dual-band rectifier utilizing a single and multi-stub matching network (MN) technique. The rectifier consists of two branches, each incorporating a single block stub and two blocks stub to generate two frequency susceptance blocks, subsequently transformed into a meandered line. The proposed rectifier operates at two frequency bands of 0.7 GHz and 0.9 GHz and is fabricated on an RT/Duroid 5880 printed circuit board (PCB) with dimensions of 37×25×1.6 mm using an entire ground architecture. Simulation and measurement results show that the rectifier has a power conversion efficiency (PCE) of 67.77% and 66.35% at 0.7 GHz and 70.31% and 71.22% at 0.9 GHz with input power of 0 dBm, respectively. The rectified voltage is 1.79 V DC across a 5 kΩ load terminal (R_L) with 5 dBm input power and is capable of sensing low input power down to -30 dBm. This feature makes the rectifier a promising solution for powering low-power devices from ambient energy.

Corresponding Author:

Mohd Najib Mohd Yasin
Faculty of Electronic Engineering and Technology, Universiti Malaysia Perlis
Arau, 02600, Perlis, Malaysia
Email: najibyasin@unimap.edu.my

1. INTRODUCTION

Radio frequency (RF) energy harvesting presents a sustainable solution for extending battery life in wireless networks, thus reducing environmental impact [1]–[3]. This technology enables low-power devices to harness RF energy from the environment or reliable sources, promoting self-sustainability and eco-friendliness [2], [4]. Unlike other renewable sources such as solar or wind, RF energy is consistently available, making it a viable option for various applications [5]. Moreover, it facilitates proactive energy replenishment for wireless devices with quality service requirements [3]. RF energy can be harvested from diverse sources including wireless internet, mobile phones, and broadcasting stations. However, challenges such as low density and efficiency, especially over long distances, need to be addressed [6]. Hence, designing an effective RF harvester with high power conversion efficiency (PCE) is challenging [7].

Over the past two decades, various rectenna designs have been investigated, including single-band and multiband rectennas, one-stage and multistage rectennas, arrays rectennas, circularly polarized rectennas, and compact rectennas for sensor networks [8], [9]. Advanced techniques, such as automatic impedance transforming, have expanded input ranges for single and dual-band rectifiers operating at 915 MHz and 915/2450 MHz, as reported in [10]. Muhammad *et al.* [7] described a 0.9 GHz and 1.8 GHz dual-band rectenna featuring a modified π-section matching network (MN). A compact dual-band four-port ambient

rectenna operating at 0.915 GHz and 0.945 GHz was demonstrated in [11]. Additionally, a compact dual-band rectifier with a single-stage T-type impedance matching network (IMN) operating at 0.915 and 2.45 GHz is presented in [12]. Researchers [13], [14] present a triple-band rectifier consisting of a single voltage doubler and a single series diode rectifier topology respectively. A compact-size quad-band rectifier consisting of a multi-stub IMN has been reported in [15].

Despite these advancements, several studies have shown that the addition of parasitic elements can degrade the rectifier's performance, leading to a larger electrical size [10], [12], [16]–[19]. For instance, the authors in [7] reported an improvement in PCE but with increased dimensions. The utilization of an MN reduces reflection losses in the antenna's RF input power [20], [21]. The diode is critical in rectifying ambient RF into direct current (DC) power [7], [22]. To eliminate harmonics generated by the diodes, a low-pass filter, known as the harmonic rejection filter (HRF), is designed and placed at the signal source's input [23], [24]. The DC-pass filter improves signal quality by removing unwanted frequencies, making power transfer more efficient and providing a steady power source [13]. The load resistor (R_L) is often complex and varies with frequency [25]. The characteristic impedance of the RF input source is typically 50 Ω [26], [27].

This paper proposes a dual-band (0.7 GHz and 0.9 GHz) efficient and compact rectenna for ambient RF energy harvesting with improved PCE. The GSM/900 frequency band is identified as a prevalent spectrum with substantial power density [7], [28], while the 700 MHz band is one of the three 5G pioneer bands in Malaysia [29]. The proposed rectifier is compact and efficient, minimizing reflection losses and harmonics through optimized impedance matching and filtering techniques. This novel approach addresses size and efficiency limitations in existing designs. The main contribution is an improved compact rectenna with high PCE for both GSM900 and 5G applications. The remainder of the report is organized as follows: section 2 covers the rectifier design, section 3 summarizes findings and discussions, and section 4 presents the conclusion.

2. METHOD

The proposed dual-band rectifier topology is depicted in Figure 1. The topology consists of an IMN, a Schottky diode, a DC-pass filter, and an R_L. The design of the rectifier was carried out on 1.575 mm thick Roger's substrates, which have a permittivity of 2.2 and a dielectric loss factor of 0.0009. The initial phase of the design process involved the simulation of the rectifier circuit using an advanced design system (ADS), which included essential components such as a diode, capacitor, and R_L. The proposed rectifier circuit aims to obtain an outstanding performance operating at 0.7 GHz, and 0.9 at low input power. To mitigate the ripple and harmonic present in the diode output, a DC-pass filter with a capacitance of 470 pF was added in parallel with R_L. Upon completing the design of the load resistance and DC pass filter, the next step involves evaluating the circuit input impedance at each operating frequency. The obtained input impedances at 0.7 GHz and 0.9 GHz are (177.316-j902.686 Ω) and (113.461-j708.086 Ω) respectively. The reason for choosing a -10 dBm input power is that the standard transceiver consistently operates below this threshold [30], [31]. Subsequently, the rectifier's input impedance is matched with the 50 Ω input source from the antenna.

The circuit topology of the rectifier, depicted in Figure 1(a) comprises key components, including a microstrip line (MLIN), a microstrip curved bend (MCURVE), a microstrip cross-junction (MCROSO), and a microstrip T-junction (MTEE). The IMN design implements a single and multi-stub matching approach, incorporating an open and shorted transmission line segment connected by TL1 and TL4, respectively, to improve the system's overall performance. Single stub and multi stub matching are employed to precisely tune the electrical length and impedance, aligning the overall system impedance with the characteristic impedance of the transmission line. This minimizes signal reflections, ensuring efficient power transfer. Single stub matching efficiently matches complex loads to characteristic impedance using a 50 Ω transmission line for both the main line and stub. Stubs, either shorted or open circuits, create pure reactance at the attachment point for the desired frequency. In microstrip board applications, parallel stub matching is preferred for its simplicity. The choice between shorted or open stubs depends on design constraints, typically favoring the topology that results in the shortest length, usually less than half a wavelength (λ), for broader bandwidth [32]. A susceptance for a single stub can be expressed by (1) and (2):

$$B_T(f_i) = -Y_T cot\theta_T(f_i), \quad \textit{(short-circuited stub)} \tag{1}$$

$$B_T(f_i) = Y_T cot\theta_T(f_i), \quad \textit{(open-circuited stub)} \tag{2}$$

where θ_T represents the electrical length of the stub at the frequency, f_i, B_T, and Y_T represent the stub susceptance and admittance operating at the frequency, f_i respectively.

In (1) and (2), a longer electrical length generally decreases susceptance magnitude. However, the specific outcome varies based on the stub type (short circuit or open circuit) and the chosen sign convention in the equation. Extending the electrical length of either the short-circuited or open-circuited stub enables finer tuning of the introduced reactive component. This facilitates achieving the desired impedance transformation and aligns the system impedance with the characteristic impedance of the transmission line. The multi-stub IMN was derived from a combination of the short and open single stub and can be expressed as (3)-(5):

$$B_T(f_i) = -Y_T cot\theta_T(f_i) - Y_T cot\theta_T(f_i), \quad (3)$$
(shorted-shorted stub)

$$B_T(f_i) = Y_T cot\theta_T(f_i) - Y_T cot\theta_T(f_i), \quad (4)$$
(open-shorted stub)

$$B_T(f_i) = Y_T cot\theta_T(f_i) + Y_T cot\theta_T(f_i), \quad (5)$$
(open-open stub)

In the proposed rectifier circuit, the single stub is a short-circuited stub represented by TL2 while the multi-stub is an open-shorted stub represented by TL5, TL6, and TL8. The use of multiple stubs gives an advantage, especially having flexibility in the tuning process to achieve the desired frequency band. The straight MLIN, which consist of TL1, TL2, TL3, TL4, TL5, TL7, TL8, and TL9, have resulted in the enlargement of the rectifier's size to 95×75 mm, as depicted in Figure 1(a). The overall circuit has been transformed into a compact design using a meandered line approach to reduce the proposed rectifier's size while maintaining a high PCE as shown in Figure 1(b). The meandered line is built using multiple sets of MLIN and MCURVE, which are arranged based on the original length of MLIN. After being transformed, the size of the proposed rectifier is 25×37 mm which is only 13% of the original size. Based on the circuit configuration in Figure 1(b), the circuit parameters of the proposed rectifier have been optimized as shown in Table 1. The proposed rectifier circuit has an overall dimension of 37×25×1.575 mm. These parameter values are chosen based on the best impedance-matching results for each branch.

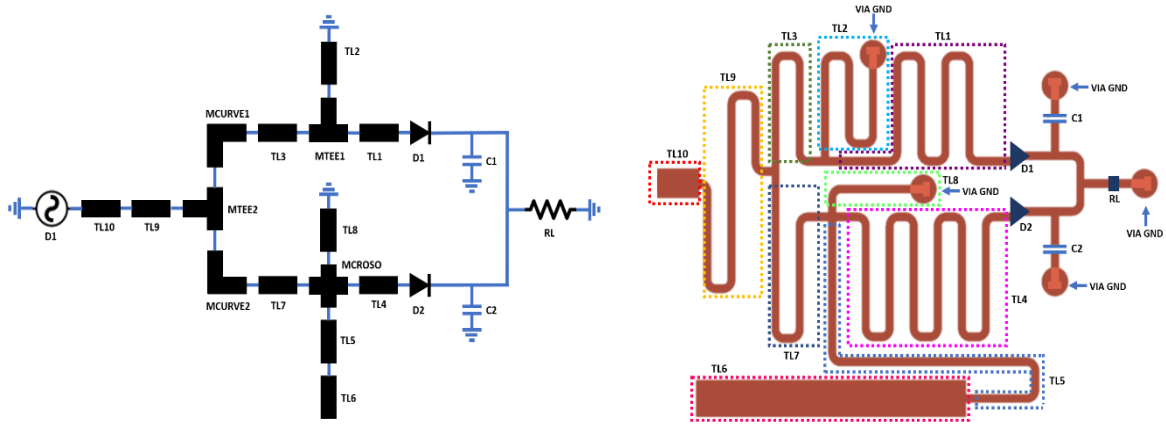

Figure 1. The proposed dual-band rectifier: (a) original model layout and (b) model layout after transformed into meandered line

The core components of a rectifier circuit are typically diodes or complementary metal-oxide-semiconductor (CMOS) technology. However, for simplicity and low input signals, Schottky diodes are preferred over CMOS due to fewer design considerations and higher efficiency at low power levels. Schottky diodes, like HSMS-2850, with a low sensitive voltage and junction capacitance, are ideal for RF applications. A single-diode design offers better efficiency and reduced energy losses compared to multi-diode setups due to the existence of additional parasitic at the junction terminals, making it suitable for stable power response at low input and high-frequency situations. The choice of the HSMS-2850 Schottky diode ensures minimal

power dissipation and efficient rectification [33]–[36]. The nonlinear properties of the rectifying diode were simulated in ADS using a parameter sweep solver and a harmonic balance (HB).

Table 1. The parameters for the rectifier circuit

Parameters	Width/length (mm)	Parameters	Width/width/width (mm)
TL1	0.6/39.74	MTEE1	0.6/0.6/0.6
TL2	0.6/20.03	MTEE2	0.6/0.6/0.6
TL3	0.6/14.6		
TL4	0.6/55.4	Parameter	Width/width/width/width (mm)
TL5	0.6/30.7	MCROSO	0.6/0.6/0.6/0.6
TL6	2.5/20.22		
TL7	0.6/21.55	Parameters	Width/radius (mm)/ (θ=90°)
TL8	0.6/27.4	MCURVE1	0.6/0.6
TL9	0.6/5.4	MCURVE2	0.6/0.6
TL10	2/3.2		

Figure 2 shows the result of the simulated PCE versus the R_L at a range of input power (P_{in}). The proposed rectifier circuit is subjected to a simulation in which the R_L is varied with an increment of 0.5 kΩ from 0.5 kΩ to 20 kΩ to determine its optimal PCE. To identify the peak value of V_{out}, a series range of R_L values is evaluated at both operating frequencies for input powers ranging from -30 dBm to 0 dBm. The simulation results show that the proposed rectifier design performed well over a wide range of R_L values, from 3.5 kΩ to 6.5 kΩ. The simulations show a better PCE throughout the 5 kΩ R_L for operating frequencies of 0.7 GHz and 0.9 GHz. The results reveal that for input powers of 0 dBm or less, the rectifier circuit produces the maximum output DC power at a load resistance of 5 kΩ.

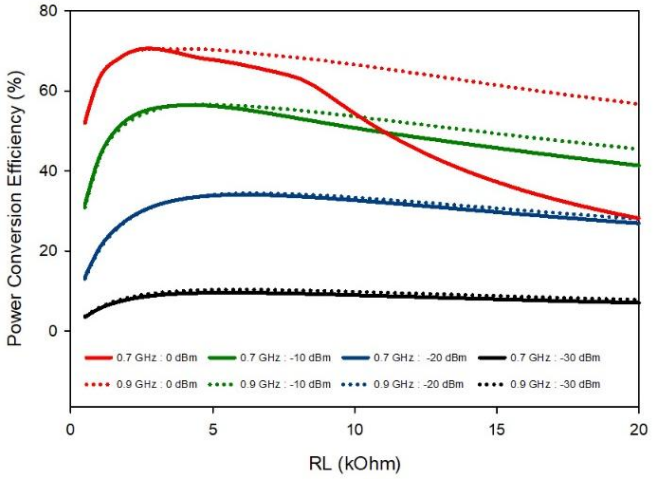

Figure 2. Simulated efficiency sweeps against R_L at the input power (Pin) range

3. RESULTS AND DISCUSSION

Figure 3(a) depicts the fabricated prototype of the proposed RF-rectifier circuit. A 50 Ω SMA port feeds the front end of the rectifier. The operating frequency of the rectifier is determined by the rectifier reflection coefficient (S11). To measure the S11 of the rectifier, a PNA network analyzer from Agilent was utilized. Figure 3(b) shows a good agreement between the simulated and measured S11, which resonates at 0.7 GHz and 0.9 GHz. In the simulation, the S11 for frequencies of 0.7 GHz and 0.9 GHz are -12.61 dB and -22.06 dB, respectively. The measured value of S11 for a frequency of 0.7 GHz is -25.3 dB which is better than simulated, while for a frequency of 0.9 GHz, the S11 value is -14.09 dB which is a bit lower than simulated.

The measurement setup for the rectified output voltage is shown in Figure 4. The rectified output voltage was measured using a multimeter, while the Rohde and Schwarz SMBV100A vector signal generator model emulated the RF signal. The RF-rectifier PCE against Pin is then evaluated by varying the input power Pin from -30 dBm to 5 dBm with a 5 dBm span for each operating frequency.

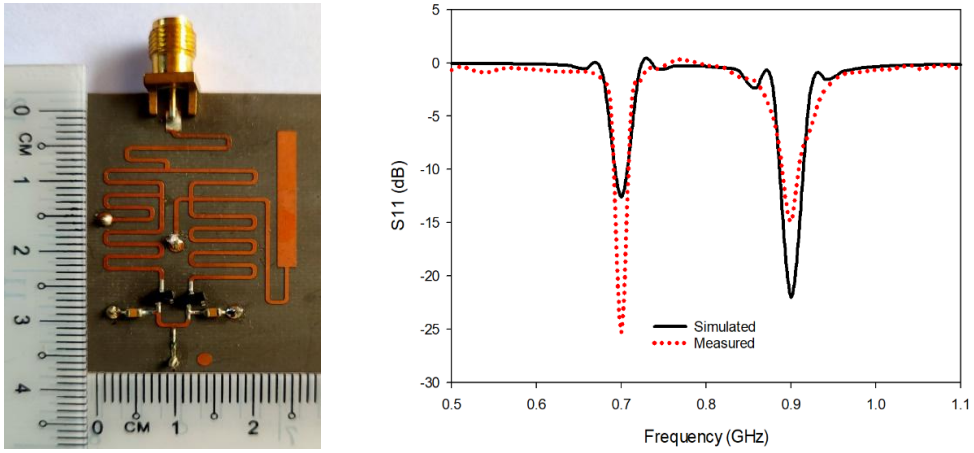

(a) (b)

Figure 3. The proposed rectifier circuit design: (a) fabricated circuit and (b) result of reflection coefficient, S11

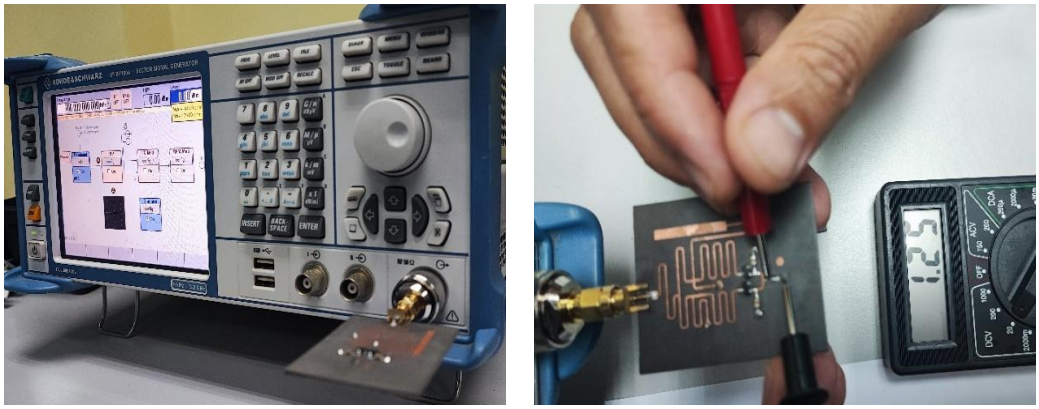

Figure 4. Measurement setup of rectified output voltage

Figure 5(a) depicts the output DC voltage (V_{dc}) versus the input power, P_{in} of the proposed rectifier. For an input range of -30 dBm to 5 dBm, the measured output voltage showed excellent agreement with the simulated results. In measurement, the circuit attained a maximum output voltage of 1.79 V and 1.72 V at 0.7 GHz and 0.9 GHz with an input power of 5 dBm, respectively. The difference between measured and simulation output voltage is only 2% and 1.74% at 0.7 GHz and 0.9 GHz bands for 0 dBm of input RF power, respectively. Figure 5(b) shows the simulated versus measured PCE of the proposed rectifier. The PCE is calculated using the measured output voltage (V_{out}), as expressed in (6):

$$\eta(\%) = P_{out}\left(\frac{1}{P_{in}}\right) X\ 100\% = V_{out}^2\left(\frac{1}{R_L\ X\ P_{in}}\right) X\ 100\% \quad (6)$$

where η represents PCE and Pout represents the rectified output power. P_{in} represents the input power. V_{out} represents the rectified output DC voltage.

As depicted in Figure 5(b), the measured result of the proposed rectifier attained a peak PCE of 66.35% and 71.22% at 0.7 GHz and 0.9 GHz with 0 dBm of input power, respectively. Meanwhile, the maximum measured PCE at -10 dBm input power is 48.01% and 58.65%, while at -20 dBm input power, the maximum PCE is 22.88% and 25.74% for 0.7 GHz and 0.9 GHz frequencies, respectively. These findings emphasize the viability of the proposed rectifier for low-power applications.

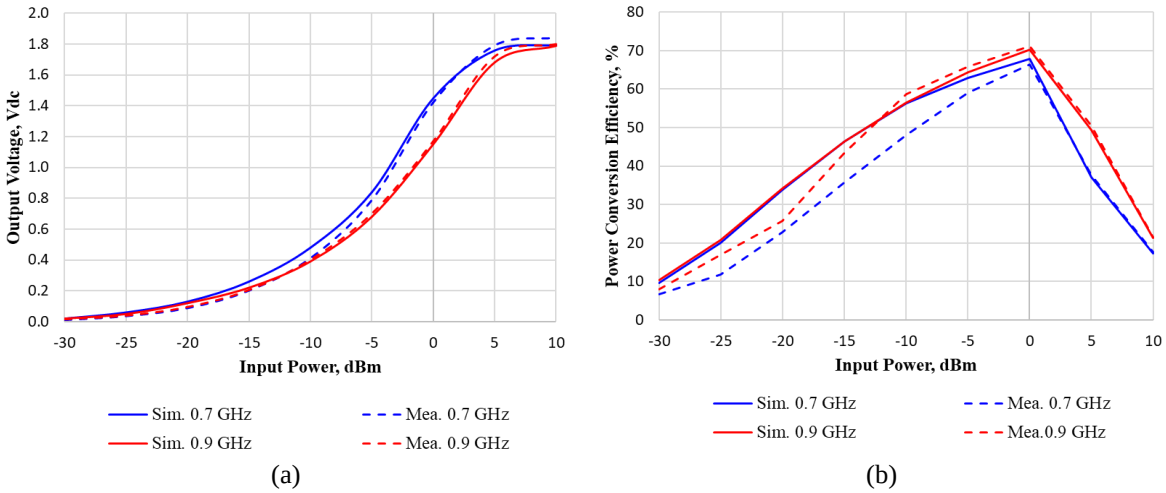

Figure 5. The results of the proposed rectifier: (a) output DC voltage versus input RF power and (b) PCE versus input RF power

Table 2 shows state of art from literature review on dual-band rectifier design. The comparison was made based on size, diode technology, the substrate used, and the efficiency of the rectifier. The proposed rectifier is superior in terms of size reduction with an improved PCE at low input power compared to the previous work reported in [7], [10], [12], [17], [19], [37], [38]. A unique feature of the proposed dual-band rectifier is its reduced circuit complexity, leading to lower parasitic effects. In comparison to other studies, the proposed design offers several advantages, such as its compact size, affordability, and ease of fabrication.

Table 2. Comparison between the previous works and the proposed dual-band rectifier

Ref.	Size (λ_g)	Freq. (GHz)	PCE (%) at -10 dBm	Substrate (ε_r)	Diode
Muhammad *et al.* [7]	0.75×0.15	0.9, 1.8	52, 50	FR-4 (5.4)	HSMS2850
Huang *et al.* [10]	0.39×0.29	0.915, 2.45	38, 22	Arlon AD255 (2.55)	HSMS2822, HSMS2852
Liu *et al.* [12]	0.35×0.17	0.9, 2.45	20, 5	Arlon AD255 (2.55)	HSMS2862
		0.9, 2.45	52, 45	Arlon AD255 (2.55)	SMS7630
Quddious *et al.* [16]	0.16×0.12	0.915, 2.45,	56, 60	RT5880 (2.2)	SMS7630
Rotenberg *et al.* [17]	0.38×0.17	1.7, 2.4	-	Taconic TLY-5 (2.2)	HSMS2828
Liu *et al.* [18]	0.18×0.09	0.915, 2.45	36, 1	Arlon AD255 (2.55)	HSMS2862
Chandravanshi *et al.* [19]	1.1×0.84	1.8, 2.45	45, 38	Polyimide (4)	SMS7630
Guo *et al.* [37]	0.63×0.31	2.6, 3.5	38, 33	RO4003C (3.55)	SMS7630-079LF
Mattsson *et al.* [38]	1.37×0.45	2.45, 5.5	20, 2	FR4 (4.5)	HSMS2852
Shen *et al.* [39]	0.18×0.08	0.9, 1.8	31, 31	RT5880 (2.2)	HSMS2850
This work	0.09×0.13	0.7, 0.9	56.24, 56.57	RT5880 (2.2)	HSM2850

Note: The PCE value at -10 dBm is estimated based on the graph presented by the authors.

4. CONCLUSION

This paper presents the compact dual-band rectifier for ambient RF energy harvesting operating at 0.7 GHz and 0.9 GHz frequency bands. The IMN of the dual-band RF rectifier is designed using a single stub and multi-stub MN, incorporating additional degrees of freedom to enhance impedance characteristics across the entire design frequency spectrum. To suit internet of thing (IoT) applications, the rectifier size has been reduced by 87% from the original size while retaining a high PCE. The proposed rectifier attained peak simulated and measured PCE values of 67.77% and 66.35% at 0.7 GHz and 70.31% and 71.22% at 0.9 GHz, correspondingly for an input power of 0 dBm. Moreover, the rectifier achieved a 1.79 V DC output voltage across a 5 kΩ R_L when subjected to 5 dBm input power. The harvested energy from the proposed rectifier can be incorporated into the new IoT-based architectures, low power wide area networks (LPAWNs).

ACKNOWLEDGEMENTS

This author would like to acknowledge the support from the Fundamental Grant Scheme (FRGS) under grant number FRGS/1/2020/TK0/UNIMAP/02/70 from the Ministry of Higher Education.

REFERENCES

[1] M. Aboualalaa and H. Elsadek, "Rectenna systems for rf energy harvesting and wireless power transfer," *Recent Wirel. Power Transf. Technol.*, pp. 1–24, 2020, doi: 10.5772/intechopen.89674.

[2] D. Khan *et al.*, "A survey on rf energy harvesting system with high efficiency rf-dc converters," *J. Semicond. Eng.*, vol. 1, no. 1, pp. 13–30, 2020, doi: 10.22895/jse.2020.0002.

[3] X. Lu, P. Wang, D. Niyato, D. I. Kim, and Z. Han, "Wireless networks with rf energy harvesting: a contemporary survey," *IEEE Commun. Surv. Tutorials*, vol. 17, no. 2, pp. 757–789, 2015, doi: 10.1109/COMST.2014.2368999.

[4] U. Muncuk, K. Alemdar, J. D. Sarode, and K. R. Chowdhury, "Multiband ambient rf energy harvesting circuit design for enabling batteryless sensors and iot," *IEEE Internet Things J.*, vol. 5, no. 4, pp. 2700–2714, 2018, doi: 10.1109/JIOT.2018.2813162.

[5] W. A. Indra and M. S. A. B. M. Shariff, "Message conveyor by motion for paralyze people powered using rf energy harvesting," *Int. J. Integr. Eng.*, vol. 12, no. 8, pp. 233–239, 2020, doi: 10.30880/IJIE.2020.12.08.022.

[6] T. Sanislav, G. D. Mois, S. Zeadally, and S. C. Folea, "Energy harvesting techniques for internet of things (iot)," *IEEE Access*, vol. 9, pp. 39530–39549, 2021, doi: 10.1109/ACCESS.2021.3064066.

[7] S. Muhammad, J. J. Tiang, S. K. Wong, A. Smida, R. Ghayoula, and A. Iqbal, "A dual-band ambient energy harvesting rectenna design for wireless power communications," *IEEE Access*, vol. 9, pp. 99944–99953, 2021, doi: 10.1109/ACCESS.2021.3096834.

[8] K. Saito, E. Nishiyama, and I. Toyoda, "A 2.45- and 5.8-ghz dual-band stacked differential rectenna with high conversion efficiency in low power density environment," *IEEE Open J. Antennas Propag.*, vol. 3, no. March, pp. 627–636, 2022, doi: 10.1109/OJAP.2022.3171035.

[9] A. Eroglu, K. Dey, R. Hussain, and T. Dey, "Design of dual band rectifiers for energy harvesting applications," *Appl. Comput. Electromagn. Soc. J.*, vol. 34, no. 2, pp. 381–384, 2019.

[10] M. Huang *et al.*, "Single-and dual-band rf rectifiers with extended input power range using automatic impedance transforming," *IEEE Trans. Microw. Theory Tech.*, vol. 67, no. 5, pp. 1974–1984, 2019, doi: 10.1109/TMTT.2019.2901443.

[11] Z. Liang and J. Yuan, "A compact dual-band four-port ambient rf energy harvester with high-sensitivity, high-efficiency, and wide power range," *IEEE Trans. Microw. Theory Tech.*, vol. 70, no. 1, pp. 641–649, 2022, doi: 10.1109/TMTT.2021.3106310.

[12] J. Liu, M. Huang, and Z. Du, "Design of compact dual-band rf rectifiers for wireless power transfer and energy harvesting," *IEEE Access*, vol. 8, pp. 184901–184908, 2020, doi: 10.1109/ACCESS.2020.3029603.

[13] H. Tafekirt, J. Pelegri-Sebastia, A. Bouajaj, and B. M. Reda, "A sensitive triple-band rectifier for energy harvesting applications," *IEEE Access*, vol. 8, pp. 73659–73664, 2020, doi: 10.1109/ACCESS.2020.2986797.

[14] S. Shen, Y. Zhang, C. Y. Chiu, and R. Murch, "A triple-band high-gain multibeam ambient rf energy harvesting system utilizing hybrid combining," *IEEE Trans. Ind. Electron.*, vol. 67, no. 11, pp. 9215–9226, 2020, doi: 10.1109/TIE.2019.2952819.

[15] S. Muhammad, J. J. Tiang, S. K. Wong, A. Smida, M. I. Waly, and A. Iqbal, "Efficient quad-band rf energy harvesting rectifier for wireless power communications," *AEU - Int. J. Electron. Commun.*, vol. 139, p. 153927, 2021, doi: 10.1016/j.aeue.2021.153927.

[16] A. Quddious, S. Zahid, F. A. Tahir, M. A. Antoniades, P. Vryonides, and S. Nikolaou, "Dual-band compact rectenna for uhf and ism wireless power transfer systems," *IEEE Trans. Antennas Propag.*, vol. 69, no. 4, pp. 2392–2397, 2021, doi: 10.1109/TAP.2020.3025299.

[17] S. A. Rotenberg, S. K. Podilchak, P. D. H. Re, C. Mateo-Segura, G. Goussetis, and J. Lee, "Efficient rectifier for wireless power transmission systems," *IEEE Trans. Microw. Theory Tech.*, vol. 68, no. 5, pp. 1921–1932, 2020, doi: 10.1109/TMTT.2020.2968055.

[18] J. Liu, X. Y. Zhang, and C. L. Yang, "Analysis and design of dual-band rectifier using novel matching network," *IEEE Trans. Circuits Syst. II Express Briefs*, vol. 65, no. 4, pp. 431–435, 2018, doi: 10.1109/TCSII.2017.2698464.

[19] S. Chandravanshi, K. K. Katare, and M. J. Akhtar, "A flexible dual-band rectenna with full azimuth coverage," *IEEE Access*, vol. 9, pp. 27476–27484, 2021, doi: 10.1109/ACCESS.2021.3058239.

[20] S. Muhammad, J. J. Tiang, S. K. Wong, A. Iqbal, M. Alibakhshikenari, and E. Limiti, "Compact rectifier circuit design for harvesting gsm/900 ambient energy," *Electron.*, vol. 9, no. 10, pp. 1–11, 2020, doi: 10.3390/electronics9101614.

[21] C. Song *et al.*, "Matching network elimination in broadband rectennas for high-efficiency wireless power transfer and energy harvesting," *IEEE Trans. Ind. Electron.*, vol. 64, no. 5, pp. 3950–3961, 2017, doi: 10.1109/TIE.2016.2645505.

[22] P. Li, Z. Long, and Z. Yang, "Rf energy harvesting for batteryless and maintenance-free condition monitoring of railway tracks," *IEEE Internet Things J.*, vol. 8, no. 5, pp. 3512–3523, 2021, doi: 10.1109/JIOT.2020.3023475.

[23] S. Saravani, C. K. Chakrabarty, N. Din, S. M. Norzeli, and M. H. Haron, "Broadband and high efficiency rectifier design based on dual-mode operation for rf ambient energy harvesting," *Int. J. Adv. Trends Comput. Sci. Eng.*, vol. 9, no. 5, pp. 7184–7190, 2020, doi: 10.30534/ijatcse/2020/43952020.

[24] S. Saravani, S. Saravani, C. K. Chakrabarty, N. Din, and S. M. Norzeli, "A novel sensitive rectifier with increased output load tolerance for ambient rf energy harvesting," *Int. J. Adv. Trends Comput. Sci. Eng.*, vol. 9, no. 5, pp. 7024–7030, 2020, doi: 10.30534/ijatcse/2020/22952020.

[25] P. Saffari, A. Basaligheh, and K. Moez, "An rf-to-dc rectifier with high efficiency over wide input power range for rf energy harvesting applications," *IEEE Trans. Circuits Syst. I Regul. Pap.*, vol. 66, no. 12, pp. 4862–4875, 2019, doi: 10.1109/TCSI.2019.2931485.

[26] J. Liu and X. Y. Zhang, "Compact triple-band rectifier for ambient rf energy harvesting application," *IEEE Access*, vol. 6, pp. 19018–19024, 2018, doi: 10.1109/ACCESS.2018.2820143.

[27] N. Saranya and T. Kesavamurthy, "Design and performance analysis of broadband rectenna for an efficient rf energy harvesting application," *Int. J. RF Microw. Comput. Eng.*, vol. 29, no. 1, 2019, doi: 10.1002/mmce.21628.

[28] S. Roy, J. J. Tiang, M. Bin Roslee, M. T. Ahmed, and M. A. P. Mahmud, "A quad-band stacked hybrid ambient rf-solar energy harvester with higher rf-to-dc rectification efficiency," *IEEE Access*, vol. 9, pp. 39303–39321, 2021, doi: 10.1109/ACCESS.2021.3064348.

[29] Malaysian Communications and Multimedia Commission, "Final report: allocation of spectrum bands for mobile broadband service in malaysia," 2019. [Online]. Available: https://www.mcmc.gov.my/skmmgovmy/media/General/pdf/PI-Allocation-of-spectrum-bands-for-mobile-broadband-service-in-Malaysia_1.pdf.

[30] Y. Luo, L. Pu, G. Wang, and Y. Zhao, "Rf energy harvesting wireless communications: rf environment, device hardware and practical issues," *Sensors (Switzerland)*, vol. 19, no. 13, 2019, doi: 10.3390/s19133010.

[31] S. K. Divakaran, D. Das Krishna, and Nasimuddin, "Rf energy harvesting systems: an overview and design issues," *Int J RF Microw Comput Aided Eng.*, vol. 29, no. 1. 2019, doi: 10.1002/mmce.21633.

[32] I. Adam, M. N. M. Yasin, M. E. A. Aziz, and M. I. Sulaiman, "Rectifier for rf energy harvesting using stub matching," *Indones. J.*

Electr. Eng. Comput. Sci., vol. 13, no. 3, pp. 1007–1013, 2019, doi: 10.11591/ijeecs.v13.i3.pp1007-1013.
[33] I. Adam, M. N. M. Yasin, S. Z. Ibrahim, and N. Haris, "Development of cascaded voltage doubler rectifier for rf energy harvesting," *J. Teknol.*, vol. 84, no. 2, pp. 153–161, 2022, doi: 10.11113/jurnalteknologi.v84.17405.
[34] S. Shen, C. Y. Chiu, and R. D. Murch, "Multiport pixel rectenna for ambient rf energy harvesting," *IEEE Trans. Antennas Propag.*, vol. 66, no. 2, pp. 644–656, 2018, doi: 10.1109/TAP.2017.2786320.
[35] K. T. Chandrasekaran, K. Agarwal, Nasimuddin, A. Alphones, R. Mittra, and M. F. Karim, "Compact dual-band metamaterial-based high-efficiency rectenna: an application for ambient electromagnetic energy harvesting," *IEEE Antennas Propag. Mag.*, vol. 62, no. 3, pp. 18–29, 2020, doi: 10.1109/MAP.2020.2982091.
[36] K. Bhatt, S. Kumar, P. Kumar, and C. C. Tripathi, "Highly efficient 2.4 and 5.8 ghz dual-band rectenna for energy harvesting applications," *IEEE Antennas Wirel. Propag. Lett.*, vol. 18, no. 12, pp. 2637–2641, 2019, doi: 10.1109/LAWP.2019.2946911.
[37] L. Guo, X. Li, W. Sun, W. Yang, Y. Zhao, and K. Wu, "Designing and modeling of a dual-band rectenna with compact dielectric resonator antenna," *IEEE Antennas Wirel. Propag. Lett.*, vol. 21, no. 5, pp. 1046–1050, 2022, doi: 10.1109/LAWP.2022.3157322.
[38] M. Mattsson, C. I. Kolitsidas, and B. L. G. Jonsson, "Dual-band dual-polarized full-wave rectenna based on differential field sampling," *IEEE Antennas Wirel. Propag. Lett.*, vol. 17, no. 6, pp. 956–959, 2018, doi: 10.1109/LAWP.2018.2825783.
[39] S. Shen, Y. Zhang, C.-Y. Chiu, and R. Murch, "An ambient rf energy harvesting system where the number of antenna ports is dependent on frequency," *IEEE Trans. Microw. Theory Tech.*, vol. 67, no. 9, pp. 3821–3832, 2019, doi: 10.1109/tmtt.2019.2906598.

BIOGRAPHIES OF AUTHORS

Raja Nor Azrin Raja Yunus is a lecturer in Electrical Engineering at the Malaysian Polytechnic and Community College Department. He received a Bachelor's degree in Electrical Engineering (Power Electronics and Drives) in 2009 and a Master of Electrical Engineering (Industrial Power) in 2014 from Universiti Teknikal Malaysia Melaka (UTeM). Currently, he is completing his Ph.D. in Communication Engineering at Universiti Malaysia Perlis (UniMAP). His research interests include antenna design and RF energy harvesting. He can be contacted at email: rajanorazrin@gmail.com.

Ismahayati Adam received a Bachelor's degree in Electrical-Electronic and Telecommunication Engineering (2006) and M.Eng. In Electronic Telecommunication Engineering (2008) from Universiti Teknologi Malaysia (UTM). She obtained her Ph.D. in Communication Engineering from Universiti Malaysia Perlis, Malaysia in 2018. Since 2008, she joined as a lecturer at the School of Computer and Communication Engineering (SCCE), currently known as the Faculty of Electronic Engineering and Technology. Her research interests include antenna design, RF energy harvesting, mutual coupling, and wireless propagation. In 2018, she received a gold medal at the International and Technology Exhibition (ITEX 2018) on RF energy harvester innovation. She is a professional technologist (Ts.) of the Malaysia Board of Technologists (MBOT). She can be contacted at email: ismahayati@unimap.edu.my.

Mohd Najib Mohd Yasin a respected scholar in Electronic Engineering, earned his M.Eng. and Ph.D. from The University of Sheffield, U.K., in 2007 and 2013. Currently a lecturer at Universiti Malaysia Perlis, Malaysia, he specializes in computational electromagnetics, conformal antennas, wireless power transfer, and array design. With a focus on dielectric resonator antennas, he demonstrates a deep commitment to modern wireless technology. Recently, he has delved into reconfigurable intelligent surfaces, an area poised to revolutionize wireless communication. He pioneering work reflects his dedication to advancing the forefront of technology, showcasing a blend of innovation, academic rigor, and a thirst for knowledge, establishing him as a distinguished figure in the field. He can be contacted at email: najibyasin@unimap.edu.my

Surajo Muhammad was born in 1984 and holds a B.Eng. degree in Computer Engineering from BUK, Nigeria, and M.Eng. degree in Electronic and Telecommunication Engineering from the UTM, JB, Malaysia, obtained in 2004 and 2014. In 2022, he completed his Ph.D. with the FOE at MMU Cyberjaya, Malaysia. Research interests: RFEH and WPT for biomedical implants, 5G, wearable, and implantable antennas. Currently, a lecturer at the Department of Electronic and Telecommunication Engineering, ABU, Zaria, Nigeria, and as a PostDoc Researcher, MMU, Malaysia. He can be contacted at email: doguwa_2002@yahoo.com.

Wan Zuki Azman Wan Muhamad is a senior lecturer at the Institute of Engineering Mathematics (IMK), Universiti Malaysia Perlis (UniMAP), Malaysia. He obtained his Doctor of Philosophy, Master's and Bachelor's degrees in the field of Applied Statistics from Universiti Teknologi Malaysia (UTM). He was recently appointed as a professional technologist (P.Tech) by the Malaysia Board of Technology (MBOT) and is also a member of the Malaysia Mathematical Sciences Society (PERSAMA). He is actively involved in teaching, research, and technical training and has published many scientific papers in High Impact Journal and Indexed journals. He can be contacted at email: wanzuki@unimap.edu.my.

Abdulrahman Amin Ahmed Ghaleb was born in Riyadh, Saudi Arabia. In 2021 he graduated from the Faculty of Electronics and Technology, University Malaysia Perlis, receiving a Bachelor's degree in Electronics Engineering. Currently works as a research assistant at the University Malaysia Perlis. Fields of research is in 5G energy harvesting. He can be contacted at email: ahmedghaleb@studentmail.unimap.edu.my.